J|A|C|S
ARTICLES
Published on Web 09/27/2006

Electronic Structure and Stability of Pentaorganosilicates

Erik P. A. Couzijn, Andreas W. Ehlers, Marius Schakel, and Koop Lammertsma*

Contribution from the Department of Organic Chemistry, Faculty of Sciences, Vrije Universiteit, De Boelelaan 1083, NL-1081 HV Amsterdam, The Netherlands

Received June 28, 2006; E-mail: k.lammertsma@few.vu.nl

Abstract: The exceptional stability of recently reported pentaorganosilicates is investigated by bond energy analyses. Experimental coupling constants are used to probe their electronic structure, entailing bonds with mixed ionic−covalent character. Our analyses reconfirm that the axial bonds are more prone to heterolytic cleavage than are the equatorial bonds. Aryl substituents provide substantial electronic stabilization by charge delocalization, but cause steric crowding due to *ortho*-hydrogen repulsion. In contrast, silicates with two ax,eq biaryl groups are not congested. The remaining substituent is confined to an equatorial site, where it is insensitive to elimination. These concepts adequately explain the experimentally observed stability trends and are valuable for designing other stable pentaorganosilicates.

Introduction

The ability of silicon to expand its valence is central to the nucleophilic activation and substitution of organosilicon compounds.[1] Many stable well-characterized pentavalent species have been reported; most carry multiple electronegative heteroatoms such as fluorine, oxygen, and/or nitrogen.[2−5] Also, hexacoordinate silicates are known such as SiF_6^{2-} and those with a SiO_6, SiN_2O_4, or SiN_2O_3C core.[3,5e,g] Tacke et al. showed that incorporating the counterion gives stable zwitterionic silicates, including the first species with SiS_2O_2C and SiS_4C skeletons,[5c,f] while others are even soluble in water.[5h] Fewer silicates are known with multiple carbon substituents due to their anticipated lower stability. The first stable hypervalent silicon hydride $H_2SiPh_3^-$ was characterized only recently.[6] For long, species with four or five carbon groups were considered to be reactive intermediates,[7] observable only in the gas phase (e.g., **1**[8b], Chart 1) or as dynamic species.[8] Illustrative is $Me_3Si(CN)_2^-Bu_4N^+$, which rapidly loses a cyano group even in the solid state.[8c] Likewise, pentaorganosilicates **2** and **3** were observed only in solution at low temperature, with **3** showing reversible loss of MeLi above −55 °C.[9] Only a few years ago, an X-ray crystal structure was reported for **4**, but this silicate decomposes above −10 °C.[10] Klumpp et al.[9b] showed spiro

Chart 1

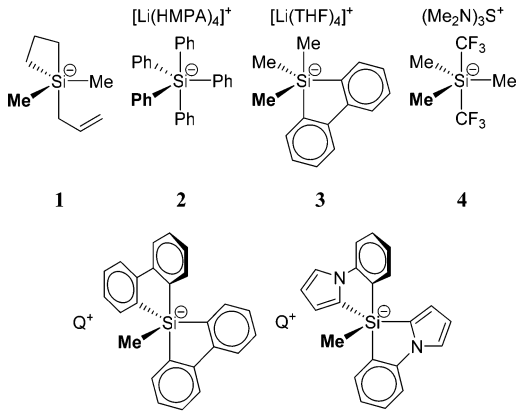

(1) Only a selection of reviews is given: (a) Bassindale, A. R.; Taylor, P. G. In *The Chemistry of Organic Silicon Compounds*; Patai, S., Rappoport, Z., Eds.; John Wiley & Sons: Chichester, UK, 1989; Part 1, pp 839−892. (b) Corriu, R. J. P.; Young, J. C. In *The Chemistry of Organic Silicon Compounds*; Patai, S., Rappoport, Z., Eds.; John Wiley & Sons: Chichester, UK, 1989; Part 2, pp 1241−1288. (c) Holmes, R. R. *Chem. Rev.* **1990**, *90*, 17−31. (d) Chuit, C.; Corriu, R. J. P.; Reye, C.; Young, J. C. *Chem. Rev.* **1993**, *93*, 1371−1448. (e) Holmes, R. R. *Chem. Rev.* **1996**, *96*, 927−950.
(2) Klüfers, P.; Kopp, F.; Vogt, M. *Chem.-Eur. J.* **2004**, *10*, 4538−4545.
(3) Wagler, J.; Böhme, U.; Brendler, E.; Thomas, B.; Goutal, S.; Mayr, H.; Kempf, B.; Remennikov, G. Y.; Roewer, G. *Inorg. Chim. Acta* **2005**, *358*, 4270−4286.
(4) Kobayashi, J.; Kawaguchi, K.; Kawashima, T. *J. Am. Chem. Soc.* **2004**, *126*, 16318−16319.
(5) (a) Tacke, R.; Pülm, M.; Wagner, B. *Adv. Organomet. Chem.* **1999**, *44*, 221−273 and references therein. (b) Kost, D.; Kalikhman, I.; Krivonos, S.; Bertermann, R.; Burschka, C.; Neugebauer, R. E.; Pülm, M.; Willeke, R.; Tacke, R. *Organometallics* **2000**, *19*, 1083−1095. (c) Tacke, R.; Mallak, M.; Willeke, R. *Angew. Chem., Int. Ed.* **2001**, *40*, 2339−2341. (d) Tacke, R.; Bertermann, R.; Burschka, C.; Dragota, S.; Penka, M.; Richter, I. *J. Am. Chem. Soc.* **2004**, *126*, 14493−14505. (e) Tacke, R.; Bertermann, R.; Burschka, C.; Dragota, S. *Z. Anorg. Allg. Chem.* **2004**, *630*, 2006−2012. (f) Seiler, O.; Büttner, M.; Penka, M.; Tacke, R. *Organometallics* **2005**, *24*, 6059−6062. (g) Seiler, O.; Burschka, C.; Metz, S.; Penka, M.; Tacke, R. *Chem.-Eur. J.* **2005**, *11*, 7379−7386. (h) Tacke, R.; Bertermann, R.; Burschka, C.; Dragota, S. *Angew. Chem., Int. Ed.* **2005**, *44*, 5292−5295.
(6) (a) Bearpark, M. J.; McGrady, G. S.; Prince, P. D.; Steed, J. W. *J. Am. Chem. Soc.* **2001**, *123*, 7736−7737. (b) Rot, N.; Nijbacker, T.; Kroon, R.; de Kanter, F. J. J.; Bickelhaupt, F.; Lutz, M.; Spek, A. L. *Organometallics* **2000**, *19*, 1319−1324.
(7) (a) Ishikawa, M.; Nishimura, K.; Sugisawa, H.; Kumada, M. *J. Organomet. Chem.* **1981**, *218*, C21−C24. (b) Ishikawa, M.; Tabohashi, T.; Sugisawa, H.; Nishimura, K.; Kumada, M. *J. Organomet. Chem.* **1983**, *250*, 109−119. (c) Tokitoh, N.; Matsumoto, T.; Suzuki, H.; Okazaki, R. *Tetrahedron Lett.* **1991**, *32*, 2049−2052. (d) Wang, Z.; Fang, H.; Xi, Z. *Tetrahedron Lett.* **2005**, *46*, 499−501.
(8) (a) DePuy, C. H.; Bierbaum, V. M.; Flippin, L. A.; Grabowski, J. J.; King, G. K.; Schmitt, R. J.; Sullivan, S. A. *J. Am. Chem. Soc.* **1980**, *102*, 5012−5015. (b) Sullivan, S. A.; DePuy, C. H.; Damrauer, R. *J. Am. Chem. Soc.* **1981**, *103*, 480−481. (c) Dixon, D. A.; Hertler, W. R.; Chase, D. B.; Farnham, W. B.; Davidson, F. *Inorg. Chem.* **1988**, *27*, 4012−4018. (d) Bushuk, S. B.; Carré, F. H.; Guy, D. M. H.; Douglas, W. E.; Kalvinkovskya, Y. A.; Klapshina, L. G.; Rubinov, A. N.; Stupak, A. P.; Bushuk, B. A. *Polyhedron* **2004**, *23*, 2615−2623.

10.1021/ja0645887 CCC: $33.50

biphenyl-substituted **5a** to be stable in solution up to +50 °C, and subsequently Lammertsma and West reported X-ray crystal structures of **5b** (mp 177−182 °C) and **5c**, respectively.[11,12] Recently, we showed that a variation of this spirosilicate **6a** with two bidentate phenylpyrrole ligands undergoes dynamic Berry pseudorotations in solution. The crystals of its *n*-Bu_4N^+ salt **6b** are highly stable (mp > 160 °C) and air-insensitive.[11b] These surprisingly stable silicates[9b] may have interesting applications, for example, as weakly coordinating counterions in ionic liquids.[13] Clearly, the exceptional stability of **5** and **6** and the special role of their biaryl ligands warrant closer scrutiny.

Pentacoordinate silicon has been the subject of theoretical studies that focused mainly on the type of bonding and the reason for the stability of SiH_5^- as compared to that of CH_5^-.[14−17] Also axial versus equatorial substitution and intramolecular ligand interchange have been addressed.[18] However, reactivity studies have been limited to possible H_2 elimination and the mechanism of nucleophilic halogen substitution at tetracoordinate silicon.[19] The influence of carbon substituents on the stability of silicates has not been investigated systematically.[20] The aim of this study is to address the electronic and steric factors that govern the thermodynamic stability of pentaorganosilicates with particular focus on the influence of the biaryl bidentates. For this purpose, we use the ADF fragment bond analysis, which provides a detailed decomposition of bond energies into physically meaningful contributions.[21]

Computational Details

General. Hybrid density-functional theory geometry optimizations were carried out with Gaussian 03[22] at the B3LYP/6-31G(d) level.[23] The easy deformability of silicates required the use of an ultrafine integration grid and tight SCF and optimization convergence criteria. The nature of each stationary point was confirmed by a frequency calculation. Reported calculated spin−spin coupling constants and bonding energy contributions are rounded to one decimal place.

Spin−Spin Coupling Constants. Single-bond NMR spin−spin coupling constants $^1J_{Si,C}$ were calculated with the Gauge-Invariant Atomic Orbital (GIAO) method at the B3LYP level. To reduce computational cost, the 6-311++G(3df,3pd) basis set was used for the coupling nuclei, 6-31G* for adjacent atoms and attached hydrogens, and 3-21G(*) for the remaining atoms.

Bonding Energy Analysis. Silicate Si−A bonds were analyzed in terms of fragment orbitals with the ADF 2004.01 package at the BP86 level using an all-electron TZP basis set and an integration accuracy of 6.0.[24] According to the extended transition-state model,[21] the net bond energy ΔE_{net} can be decomposed into four contributions (Figure 1): the preparation energy ΔE_{prep} required for deformation of the fragments from their equilibrium structure to their geometry in the silicate; the steric interactions between the fragments due to Pauli repulsion (ΔE_{Pauli}) and electrostatic attraction (ΔV_{elstat}); and the orbital interaction energy ΔE_{oi} (negative, stabilizing):

$$\Delta E_{net} = E_{silicate} - (E_{silane} + E_{anion}) = \Delta E_{prep} + (\Delta E_{Pauli} + \Delta V_{elstat} + \Delta E_{oi}) \quad (1)$$

The latter three contributions are usually summed to give the interaction energy ΔE_{int}.

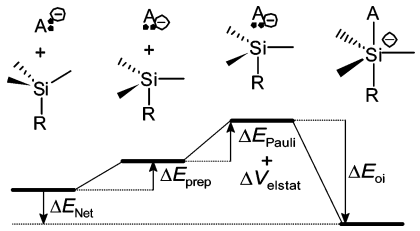

Figure 1. Bond energy decomposition.

Results and Discussion

We first discuss the general electronic structure of silicates to obtain a framework for the interpretation of the bond strength decomposition. Experimental results have indicated that the reactivity of pentaorganosilicates is governed by their ability to cleave an axial bond heterolytically.[7,9b] Therefore, we analyze the axial Si−H bond strength in monoorganosilicates SiH_4R^- (R = Me, Ph, C≡CH, CF_3) to address the electronic influence of organic substituents. We also treat the effect of the orientation of the aryl group in terms of repulsion between the axial bonds and the aromatic π system. This indirect strategy allows for a comparison of the effect of multiple (two) aryl substitution against that of the biphenyl moiety. A direct Si−C bond analysis would be complicated by the difference in stabilities of the R^- carbanion fragments and would not be extendible to bidentate substituents, as it would not result in the proper division of the silicate into silane and carbanion fragments. Subsequently, steric and conformational effects in pentaorganosilicates are addressed.

(9) (a) de Keijzer, A. H. J. F.; de Kanter, F. J. J.; Schakel, M.; Schmitz, R. F.; Klumpp, G. W. *Angew. Chem., Int. Ed. Engl.* **1996**, *35*, 1127−1128. (b) de Keijzer, A. H. J. F.; de Kanter, F. J. J.; Schakel, M.; Osinga, V. P.; Klumpp, G. W. *J. Organomet. Chem.* **1997**, *548*, 29−32.
(10) Kolomeitsev, A.; Bissky, G.; Lork, E.; Movchun, V.; Rusanov, E.; Kirsch, P.; Röschenthaler, G.-V. *Chem. Commun.* **1999**, 1017−1018.
(11) (a) Deerenberg, S.; Schakel, M.; de Keijzer, A. H. J. F.; Kranenburg, M.; Lutz, M.; Spek, A. L.; Lammertsma, K. *Chem. Commun.* **2002**, 348−349. (b) Couzijn, E. P. A.; Schakel, M.; de Kanter, F. J. J.; Ehlers, A. W.; Lutz, M.; Spek, A. L.; Lammertsma, K. *Angew. Chem., Int. Ed.* **2004**, *43*, 3440−3442.
(12) Ballweg, D.; Liu, Y.; Guzei, I. A.; West, R. *Silicon Chem.* **2002**, *1*, 55−58.
(13) (a) *Ionic Liquids in Synthesis*; Wasserscheid, P., Welton, T., Eds.; Wiley−VCH: Weinheim, Germany, 2003. (b) Rogers, R. D.; Seddon, K. R. *Science* **2003**, *302*, 792−793.
(14) (a) Hoffmann, R.; Howell, J. M.; Muetterties, E. L. *J. Am. Chem. Soc.* **1972**, *94*, 3047−3058. (b) Rauk, A.; Allen, L. C.; Mislow, K. *J. Am. Chem. Soc.* **1972**, *94*, 3035−3040. (c) Gimarc, B. M. *J. Am. Chem. Soc.* **1978**, *100*, 2346−2353.
(15) (a) Magnusson, E. *J. Am. Chem. Soc.* **1990**, *112*, 7940−7951. (b) Reed, A. E.; Schleyer, P. v. R. *J. Am. Chem. Soc.* **1990**, *112*, 1434−1445. (c) Cooper, D. L.; Cunningham, T. P.; Gerratt, J.; Karadakov, P. B.; Raimondi, M. *J. Am. Chem. Soc.* **1994**, *116*, 4414−4426.
(16) Carroll, M. T.; Gordon, M. S.; Windus, T. L. *Inorg. Chem.* **1992**, *31*, 825−829.
(17) Bento, A. P.; Bickelhaupt, F. M., personal communication.
(18) (a) Windus, T. L.; Gordon, M. S.; Davis, L. P.; Burggraf, L. W. *J. Am. Chem. Soc.* **1994**, *116*, 3568−3579. (b) Damrauer, R.; Burggraf, L. W.; Davis, L. P.; Gordon, M. S. *J. Am. Chem. Soc.* **1988**, *110*, 6601−6606. (c) Schmidt, M. W.; Windus, T. L.; Gordon, M. S. *J. Am. Chem. Soc.* **1995**, *117*, 7480−7486. (d) Deiters, J. A.; Holmes, R. R. *Organometallics* **1996**, *15*, 3944−3956. (e) Pülm, M.; Tacke, R. *Organometallics* **1997**, *16*, 5664−5668.
(19) (a) Moc, J. *J. Mol. Struct. (THEOCHEM)* **1999**, *461*, 249−259. (b) Deiters, J. A.; Holmes, R. R. *J. Am. Chem. Soc.* **1987**, *109*, 1692−1696. (c) Deiters, J. A.; Holmes, R. R. *J. Am. Chem. Soc.* **1990**, *112*, 7197−7202.
(20) $SiX_3Cl_2^-$ (X = Cl, Me) species have been compared: Hao, C.; Kaspar, J. D.; Check, C. E.; Lobring, K. C.; Gilbert, T. M.; Sunderlin, L. S. *J. Phys. Chem. A* **2005**, *109*, 2026−2034.
(21) (a) Morokuma, K. *Acc. Chem. Res.* **1977**, *10*, 294−300. (b) Ziegler, T.; Rauk, A. *Inorg. Chem.* **1979**, *18*, 1755−1759. (c) Ziegler, T.; Rauk, A. *Theor. Chim. Acta* **1977**, *46*, 1−10. (d) Bickelhaupt, F. M.; Baerends, E. J. In *Reviews in Computational Chemistry*; Lipkowitz, K. B., Boyd, D. B., Eds.; Wiley: New York, 2000; Vol. 15, pp 1−86.
(22) Frisch, M. J.; et al. *Gaussian 03*, revision B.05; Gaussian, Inc.: Wallingford, CT, 2004.
(23) (a) Becke, A. D. *J. Chem. Phys.* **1993**, *98*, 5648−5652. (b) Lee, C.; Yang, W.; Parr, R. G. *Phys. Rev. B* **1988**, *37*, 785−789.
(24) (a) te Velde, G.; Bickelhaupt, F. M.; Baerends, E. J.; Fonseca Guerra, C.; van Gisbergen, S. J. A.; Snijders, J. G.; Ziegler, T. Chemistry with ADF. *J. Comput. Chem.* **2001**, *22*, 931−967. (b) Fonseca Guerra, C.; Snijders, J. G.; te Velde, G.; Baerends, E. J. *Theor. Chem. Acc.* **1998**, *99*, 391−403. (c) ADF2004.01, SCM, Theoretical Chemistry, Vrije Universiteit, Amsterdam, The Netherlands, http://www.scm.com.

Table 1. Experimental and Calculated $^1J_{Si,C}$ (Hz) of Pentaorganosilicates **5** and **6**

	C	$^1J_{Si,C}^{exp}$	$^1J^{calc}$ =	FC +	SD +	PSO +	DSO
5	ax	33.4	28.8	28.8	0.9	−1.0	0.2
	eq	70.1	67.6	67.5	1.2	−1.3	0.2
	Me	57.4	53.3	52.7	1.4	−0.9	0.1
6	ax	30	24.4	24.2	0.9	−0.8	0.2
	eq	86	86.3	86.8	0.9	−1.6	0.2
	Me	64	60.4	59.8	1.3	−0.9	0.1

Finally, we apply these concepts to explain the remarkable thermodynamic stability of **5** and **6**.

Electronic Structure. A still popular model for pentavalent compounds was first proposed by Pimentel and by Rundle.[25] It comprises three Si-sp^2 hybrid orbitals for the equatorial bonds, which would thus be short, with the remaining Si-p_z orbital participating in an ionic 3 center-4 electron (3c-4e) interaction, giving much longer bonds with the axial substituents. However, this picture conflicts with the observed rather similar axial and equatorial Si−C bond lengths in the crystal structures of **5b**,**c** and **6b**.[11,12]

The electronic structure of pentaorganosilicates can be probed experimentally by analysis of the NMR Si−C single-bond spin−spin coupling constants $^1J_{Si,C}$, which originate from the Fermi Contact (FC), spin-dipole (SD), paramagnetic spin−orbit (PSO), and diamagnetic spin−orbit (DSO) interaction mechanisms.[26] Of these, the FC coupling relates to spin polarization of the valence electrons and is proportional to the s contributions of the nuclei to their mutual bond.[26b,27] Table 1 shows excellent agreement of the experimental $^1J_{Si,C}$ for **5** and **6**[9b,11b] with the calculated values that are by far dominated by the FC coupling. It is apparent from the experimental $^1J_{Si,C}$ values that the axial bonds contain considerable Si−C s interaction, in fact, to the amount of 35−50% of that of the equatorial bonds, which is in sharp contrast to the 3c-4e model. The equatorial Si−Me coupling is about 75% of the Si−C_{eq} coupling, reflecting the different carbon hybridization (sp^3 versus sp^2).

To analyze the orbital interactions, we apply a symmetry-adapted MO model for the silicates as proposed by Muetterties and by Mislow for PH_5 (Figure 2).[14] The HOMO is essentially located on all five substituents, thereby contributing to the ionic character of the bonds. The remaining four bonding MOs describe the covalent part of the five bonds. The axial bonds are less covalent than the equatorial ones, as illustrated by the relative contributions of the orbital coefficients in the $3a_1'$ MO; the 1:2 ratio is consistent with the noted $^1J_{Si,C}$ for **5** and **6**. This MO model, giving similar axial and equatorial bonds, is compatible with one-center expansion techniques[28a] and population analyses based on AIM.[28b,c] Also, valence-bond calculations on the stability of SiH_5^- indicated that the s interaction in the axial bonds is essential and more important than 3c-4e bonding.[28d]

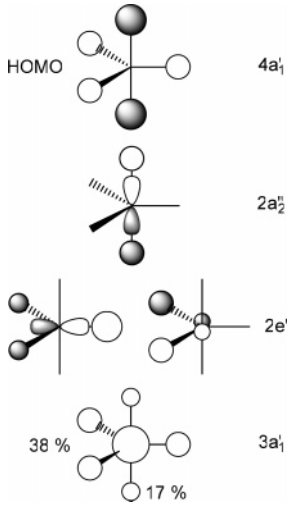

Figure 2. SiH_5^- valence MO diagram.

Table 2. Bond Analyses for SiH_5^- (kcal mol^{-1})

	ax	eq
ΔE_{Pauli}	193.9	213.3
ΔV_{elstat}	−127.6	−144.5
ΔE_{oi}	−114.7	−149.7
ΔE_{int}	−48.4	−80.8
ΔE_{prep}	21.9	54.3
ΔE_{net}	−26.5	−26.5

A similar picture emerges from the energy decomposition of the interaction between the hydride anion and the SiH_4 fragment in the geometry of the silicate. Table 2 lists the components for the axial (ax) and equatorial (eq) bonds of SiH_5^-. In line with experiment, the axial bond is predicted to be more prone to heterolytic cleavage, as apparent from its much smaller interaction energy ΔE_{int} of 48.4 (ax) versus 80.8 kcal mol^{-1} (eq). The principal difference lies in the 35.0 kcal mol^{-1} stronger orbital interaction for the equatorial bond, which is due to the much lower LUMO of the pro-equatorial SiH_4 fragment (−3.923 eV) as compared to that of the pro-axial SiH_4 fragment (−2.034 eV). The larger electrostatic attraction results from the slightly shorter bond length (1.543 Å (eq) vs 1.618 Å (ax)) and is countered by a similar increase in Pauli repulsion. The ratios between ΔE_{oi} and ΔV_{elstat} of 1.04 (eq) and 0.90 (ax) reflect the slightly more covalent nature of the equatorial bonds.

Electronic Substituent Effect. Apicophilicity. We turn to the effect of introducing different (**7**-R, **8**-R; R = Me, Ph, C≡CH, CF_3) and multiple (**9**−**12**) carbon substituents (Chart 2). Of the investigated monosubstituted silicates, the Si−C bond is slightly longer for an axial substituent (**7**-R) than for an equatorial one (**8**-R). In all cases, those with an axial group are the more stable ones. The preference of axial over equatorial substitution (apicophilicity) increases with the electron-withdrawing nature of the substituent, from 0.4 kcal mol^{-1} for R = Me to a substantial 9.3 kcal mol^{-1} for R = CF_3. Unexpectedly, in the case of a phenyl group, the energy difference between the two minima (i.e., **7**-Ph$^{\perp}$ and **8**-Ph$^{\perp}$) is merely 0.6 kcal mol^{-1}.

(25) (a) Pimentel, G. C. *J. Chem. Phys.* **1951**, *19*, 446−448. (b) Rundle, R. E. *J. Am. Chem. Soc.* **1963**, *85*, 112−113. (c) Musher, J. I. *Angew. Chem., Int. Ed. Engl.* **1969**, *8*, 54−68. (d) Musher, J. I. *J. Am. Chem. Soc.* **1972**, *94*, 1370−1371. (e) Hajdasz, D. J.; Ho, Y.; Squires, R. R. *J. Am. Chem. Soc.* **1994**, *116*, 10751−10760. (f) Moc, J.; Morokuma, K. *J. Mol. Struct.* **1997**, *436*−*437*, 401−418. (g) Cheung, Y.-S.; Ng, C.-Y.; Chiu, S.-W.; Li, W.-K. *J. Mol. Struct. (THEOCHEM)* **2003**, *623*, 1−10.

(26) (a) Ramsey, N. F. *Phys. Rev.* **1953**, *91*, 303−307. (b) Ramsey, N. F.; Purcell, E. M. *Phys. Rev.* **1952**, *85*, 143−144.

(27) (a) Summerhays, K. D.; Deprez, D. A. *J. Organomet. Chem.* **1976**, *118*, 19−25. (b) Wu, A.; Gräfenstein, J.; Cremer, D. *J. Phys. Chem. A* **2003**, *107*, 7043−7056. (c) Della, E. W.; Tsanaktsidis, J. *Organometallics* **1988**, *7*, 1178−1182. (d) Popelis, Y.; Lukevits, E. *Chem. Heterocycl. Compd.* **1993**, *29*, 744−753. (e) Müller, T.; Juhasz, M.; Reed, C. A. *Angew. Chem., Int. Ed.* **2004**, *43*, 1543−1546.

(28) (a) Häser, M. *J. Am. Chem. Soc.* **1996**, *118*, 7311−7325. (b) Molina, J. M.; Dobado, J. A. *Theor. Chem. Acc.* **2001**, *105*, 328−337. (c) Ponec, R.; Yuzhakov, G.; Cooper, D. L. *Theor. Chem. Acc.* **2004**, *112*, 419−430. (d) Sini, G.; Ohanessian, G.; Hiberty, P. C.; Shaik, S. S. *J. Am. Chem. Soc.* **1990**, *112*, 1407−1413.

Chart 2. Optimized Silicate Structures with Selected Bond Lengths (Å), BP86/TZP Relative Energy (kcal mol^{-1}), Point Group, and Number of Imaginary Frequencies in Parentheses[a]

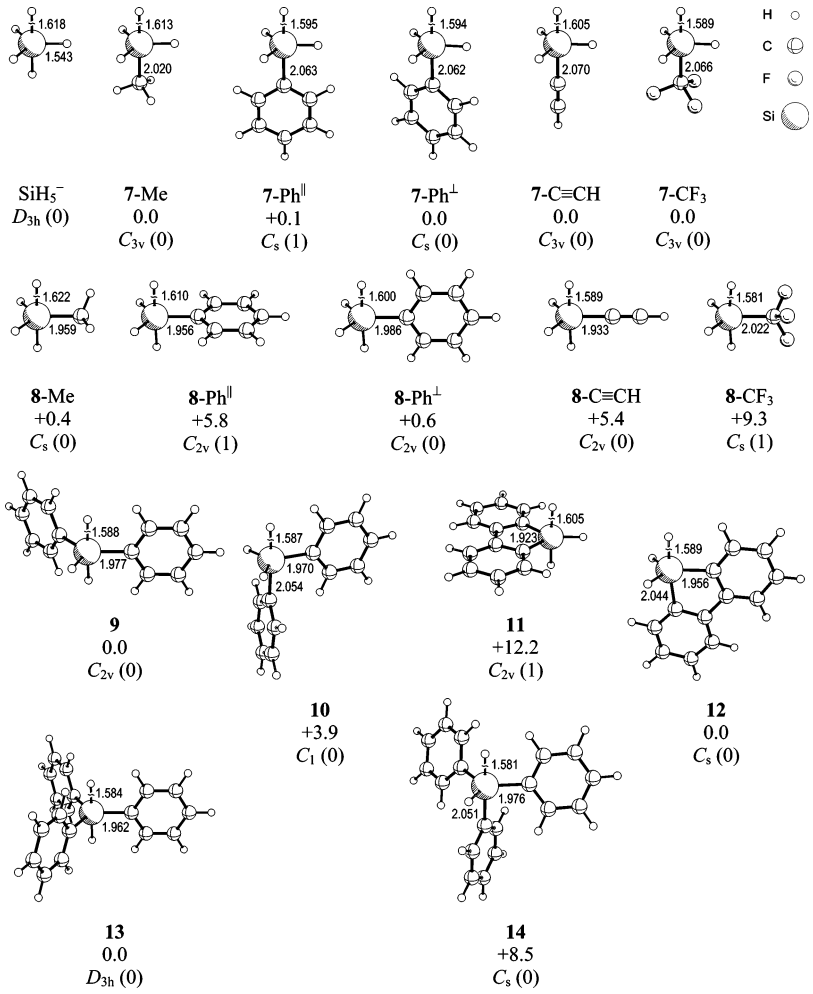

SiH_5^- D_{3h} (0)

7-Me 0.0 C_{3v} (0)

7-Ph$^{||}$ +0.1 C_s (1)

7-Ph$^{\perp}$ 0.0 C_s (0)

7-C≡CH 0.0 C_{3v} (0)

7-CF_3 0.0 C_{3v} (0)

8-Me +0.4 C_s (0)

8-Ph$^{||}$ +5.8 C_{2v} (1)

8-Ph$^{\perp}$ +0.6 C_{2v} (0)

8-C≡CH +5.4 C_{2v} (0)

8-CF_3 +9.3 C_s (1)

9 0.0 C_{2v} (0)

10 +3.9 C_1 (0)

11 +12.2 C_{2v} (1)

12 0.0 C_s (0)

13 0.0 D_{3h} (0)

14 +8.5 C_s (0)

[a] For R = Ph, superscript || (⊥) denotes an eclipsed (staggered, **7**-Ph) or a parallel (perpendicular, **8**-Ph) orientation of the ring relative to the equatorial bonds.

Table 3. Axial Si−H Bond Analyses for Monosubstituted Silicates (kcal mol^{-1})

	7-R (axial)					**8**-R (equatorial)				
R	Me	Ph$^{||}$	Ph$^{\perp}$	C≡CH	CF_3	Me	Ph$^{||}$	Ph$^{\perp}$	C≡CH	CF_3
ΔE_{Pauli}	197.1	199.4	199.6	189.7	197.1	190.7	199.4	208.3	207.5	217.9
ΔV_{elstat}	−126.4	−132.7	−132.9	−136.7	−146.2	−132.0	−135.0	−144.0	−140.4	−159.0
ΔE_{oi}	−121.8	−130.7	−131.1	−120.7	−127.9	−109.2	−118.9	−125.2	−127.3	−131.4
ΔE_{int}	−51.1	−64.0	−64.4	−67.7	−76.9	−50.5	−54.5	−60.8	−60.3	−72.5
ΔE_{prep}	25.0	27.7	28.0	28.6	21.5	24.9	23.8	25.0	26.7	26.4
ΔE_{net}	−26.0	−36.3	−36.4	−39.0	−55.4	−25.6	−30.7	−35.8	−33.6	−46.1

The apicophilicity is reflected in the Si−H bond energies (ΔE_{net}, Table 3) for **7**-R and **8**-R, which have the same silane SiH_3R as reference. The Si−H bond energy decompositions of the monosubstituted silicates are given in Table 3. The strength of the axial Si−H bond is affected considerably by substitution, especially in the (opposite) axial position. Highly electron-withdrawing groups provide the strongest stabilization, up to 28.9 kcal mol^{-1} (R = CF_3) relative to **7**-H. This is mainly an electrostatic effect, as is apparent from the linear correlation of ΔV_{elstat} with the net axial Si−H bond energy (Figure 3, r^2 = 0.984 (**7**) and 0.937 (**8**)). The influence of the orbital interaction and Pauli repulsion terms is much stronger for the equatorial substituents (**8**-R) than for the axial ones.

We next focus on the electronic influence of the experimentally more interesting phenyl group followed by that of a biphenyl group.

Phenyl Orientation. The phenyl group can be oriented either parallel (Ph$^{||}$) or perpendicular (Ph$^{\perp}$) to the equatorial Si−H bonds, which may obscure the true substituent effect. We use the same identifiers Ph$^{||}$ and Ph$^{\perp}$ for the eclipsed and staggered conformers of **7**-Ph, respectively. An axial phenyl substituent strengthens the opposite (axial) Si−H bond by 9.9 versus 28.9 kcal mol^{-1} for CF_3. While the bond energy is hardly affected by the orientation of the axial phenyl group (**7**-Ph$^{||}$ versus **7**-Ph$^{\perp}$), there is a 5.2 kcal mol^{-1} difference (rotation barrier) for the equatorial phenyl group that favors the perpendicular conformer

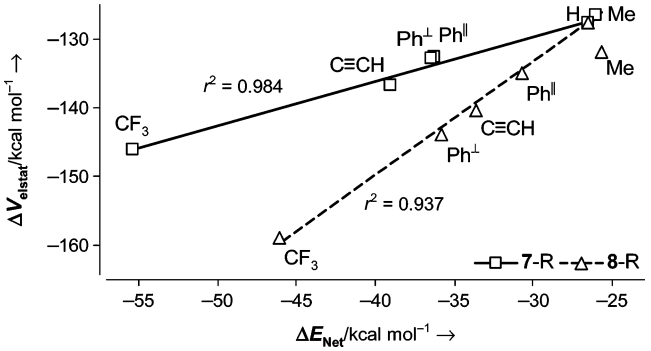

Figure 3. Electrostatic contribution plotted against net axial Si−H bond energy in monosubstituted silicates, using data from Table 3. Least-squares linear fits were enforced to cross at SiH_5^- (R = H, values from Table 2).[29]

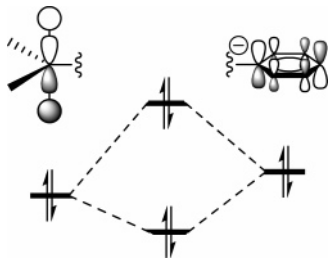

Figure 4. π repulsion MO diagram for **8**-Ph$^{\parallel}$.

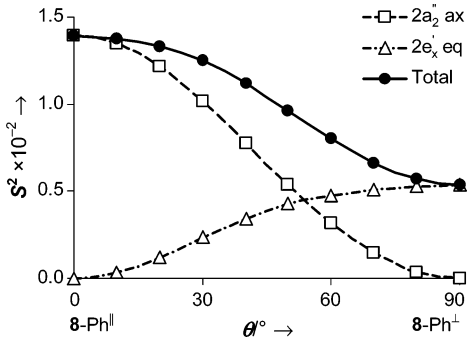

Figure 5. Squared overlaps between phenyl-π and axial (ax) and equatorial (eq) Si−H bond orbitals for **8**-Ph Si−C bond rotation. θ is the angle between the phenyl ring plane and the equatorial plane.

8-Ph$^{\perp}$. This difference is largely caused by the balance of the repulsive interactions between the phenyl π system and the occupied $2a_2''$ (Si-p_z) and 2e′ (Si-p_x) orbitals of the silicate (Figure 4).[14a] The effect can be quantified for the Si−Ph bond in terms of overlap (S) of its fragment orbitals (see Supporting Information). The amount of π repulsion is governed by the degree of overlap as illustrated in Figure 5, where S^2 is plotted as a function of the Si−Ph bond rotation (θ) of **8**-Ph. The aromatic π system in the more stable **8**-Ph$^{\perp}$ ($\theta = 90°$) overlaps less with the 2e′ (Si-p_x) silane orbital, which is directed away to the opposite H_{eq} atoms, than it does in the less stable **8**-Ph$^{\parallel}$ ($\theta = 0°$) with the axially oriented $2a_2''$ orbital. In the axially substituted **7**-Ph, the repulsion between the 2e′ orbitals and the aromatic ring is independent of its orientation and is of a magnitude that is intermediate between that of **8**-Ph$^{\perp}$ and **8**-Ph$^{\parallel}$. The surprising net effect is that the phenyl group is apico-indifferent despite its electron-withdrawing nature.

Biphenyl Bidentate Substituent. In this section, we analyze the electronic influence of disubstitution for the silicates **9** and **10**, which have phenyl groups in respectively eq$^{\perp}$,eq$^{\perp}$ and ax$^{\perp}$,eq$^{\perp}$ (all Ph$^{\perp}$) positions, and **11** and **12**, which have correspondingly eq$^{\parallel}$,eq$^{\parallel}$ and ax$^{\parallel}$,eq$^{\perp}$ biphenyl groups. The relative energies, favoring **9** and **12**, illustrate a reversal of apicophilicity for the diphenyl derivative and instead a greatly enhanced preference for axial substitution for the biphenyl derivative. In fact, **11** is the transition structure for ax,eq interchange of its biphenyl group with a substantial barrier of 12.2 kcal mol^{-1}.

Table 4. Axial Si−H Bond Analyses of Di- and Trisubstituted Silicates (kcal mol^{-1})

	9	**10**	**11**	**12**	**13**	**14**
ΔE_{Pauli}	219.5	216.3	204.4	206.1	228.5	228.6
ΔV_{elstat}	−159.8	−148.3	−143.4	−144.4	−173.8	−162.5
ΔE_{oi}	−131.2	−137.2	−122.1	−133.0	−133.0	−139.9
ΔE_{int}	−71.6	−69.1	−61.0	−71.3	−78.4	−73.8
ΔE_{prep}	28.4	29.9	27.0	25.0	29.1	33.0
ΔE_{net}	−43.2	−39.3	−34.1	−46.3	−49.3	−40.8

The additional substituent strengthens the axial Si−H bond in both types of silicates (Table 4). For example, the interaction energy ΔE_{int} increases from −48.4 (**7**-H, SiH_5^-) to −60.8 (**8**-Ph$^{\perp}$) to −71.6 (**9**) kcal mol^{-1} on successive phenyl substitution, which amounts to about 12 kcal mol^{-1} per phenyl group. Again, the main contribution comes from the electrostatic interaction. The interaction energies of **9**, **10**, and **12** are similar, while that of **11** is 10 kcal mol^{-1} smaller because of the two destabilizing π interactions with the axial bonds. Thus, the electronic stabilization and therefore the electron-withdrawing ability of the biphenyl groups in **11** and **12** are very similar to those of two separate Ph substituents. In these structures, the C−Si−C angle strain (i.e., 90.2° in **11** versus 120° in SiH_5^-) appears to be minor as the deformation energies ΔE_{prep} for **11** (27.0 kcal mol^{-1}) and the ax,eq-biphenyl substituted **12** (25.0 kcal mol^{-1}) are similar. On the other hand, the deformation energy is larger for silicate **10** (29.9 kcal mol^{-1}) due to steric repulsion between Ph_{ax} and the *ortho*-H atom of Ph_{eq}.

Steric and Conformational Effects. We first investigate the steric effects in silicates **13** and **14**, which carry three phenyl groups in respectively eq$^{\perp}$,eq$^{\perp}$,eq$^{\perp}$ and ax$^{\parallel}$,eq$^{\perp}$,eq$^{\perp}$ positions. The experimentally known conformer **13**[6] is preferred over **14** by a considerable 8.5 kcal mol^{-1}. Both equatorial Ph substituents in **14** make an angle $\theta = 63°$ with the equatorial plane to diminish *ortho*-hydrogen repulsion with the axial Ph.

The effect of this bond rotation becomes apparent from the axial Si−H bond analyses of **13** and **14** (Table 4). The extra phenyl group in **13** further enhances the interaction energy, and as a result the axial Si−H bond is 49.3 kcal mol^{-1} strong. Conversely, in **14** the deviation of both Ph_{eq}'s by 27° from the preferred Ph$^{\perp}$ orientation causes an increase in π repulsion, as expressed in the reduced electrostatic attraction, and this counters the extra stabilization of the third Ph. Also, the steric crowding is larger, as is apparent from the deformation energy ΔE_{prep} of 33.0 versus 29.1 kcal mol^{-1} for **13**. As a result, the total axial Si−H bond energy is even smaller than that of diphenylsilicate **9** (40.8 vs 43.2 kcal mol^{-1}, respectively).

Next, we focus on fully substituted silicates that carry four phenyl (**15**) or two biphenyl substituents (**5**) and an additional axial (**A**) or equatorial (**E**) methyl group to reflect the experimentally known system **5** (Chart 3). Particularly for the tetraphenyl derivative, the higher substitution pattern enhances the steric crowding that was already evident for the di- and

Chart 3. Pentaorganosilicate Structures with Equatorial Aryl Bond Rotation Angles θ, Si−Me Bond Lengths (Å), BP86/TZP Relative Energy (kcal mol^{-1}), Point Group, and Number of Imaginary Frequencies in Parentheses

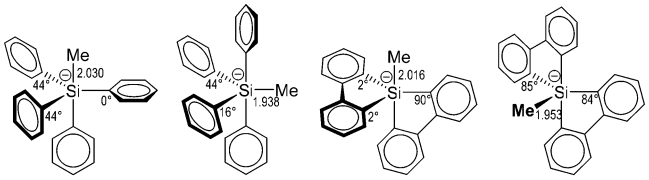

15A	**15E**	**5A**	**5E**
+1.4	0.0	+9.5	0.0
C_s (0)	C_1 (0)	C_s (1)	C_1 (0)

Table 5. Si−Me Bond Analyses of Pentaorganosilicates (kcal mol^{-1})

	15A	**15E**	**5A**	**5E**
ΔE_{Pauli}	241.9	283.2	242.1	266.3
ΔV_{elstat}	−188.8	−225.6	−193.3	−213.7
ΔE_{oi}	−135.3	−176.3	−135.4	−163.7
ΔE_{int}	−82.2	−118.8	−86.5	−111.1
ΔE_{prep}	38.4	73.6	34.1	49.1
ΔE_{net}	−43.7	−45.2	−52.4	−62.0

trisubstituted silicates. Now conformer **15E** with phenyl groups in both axial sites is slightly favored over **15A** ($\Delta E = 1.4$; $\Delta E^{\ddagger} = 2.0$ kcal mol^{-1}). With two biphenyl groups the apicophilicity remains enhanced, as for **12**, with a 9.5 kcal mol^{-1} preference for **5E**. Each of its bidentate ligands occupies an axial−equatorial position, and as a result the methyl group resides in the remaining equatorial position. Actually, like **11**, **5A** with an axial methyl group is the transition structure for a Berry pseudorotation that interconverts the silicate's ligands.[30,31]

We analyze the four structures with respect to the strength of the Si−Me bond (ax and eq) and its energy decomposition (Table 5). The equatorial Si−Me bonds have much larger interaction energies ΔE_{int}, reflecting stronger bonding, than the axial ones. Whereas the preparation energy may suggest only slightly more steric congestion for **15A** than for **5A**, the axial Si−Me bond of **15A** is weaker by as much as 8.7 kcal mol^{-1}. In fact, all three equatorial phenyl substituents are distorted from their preferred Ph$^{\perp}$ orientation with one even rotated by 90° (Ph$^{\parallel}$) to diminish the steric repulsion of their *ortho*-hydrogen atoms with the axial substituents. The increased π repulsion weakens the axial bonds, as expressed in the reduced Si−Me electrostatic attraction, and as a result the Si−Me bond of only 43.7 kcal mol^{-1} does not benefit from the higher substitution pattern of the silicate. For **15E**, the π repulsion is already present in the equatorially deformed silane fragment, resulting in a much larger ΔE_{prep} of 73.6 versus 54.3 kcal mol^{-1} for SiH_5^- (Table 2). In contrast, the Si−Me bond energy decomposition of **5E** with its two bidentate ligands reflects no steric strain at all. For an equatorial bond, the ΔE_{prep} of 49.1 kcal mol^{-1} is rather low. The orbital interaction of −163.7 kcal mol^{-1} is somewhat smaller than that in **15E** (−176.3 kcal mol^{-1}) due to a reduction in overlap. Yet the Si−Me bond for **5E** is as much as 62.0 kcal mol^{-1} strong as a result of the accumulated substituent effects.

Comparison with Experimental Data

The theoretical analyses provide important insights into the observed pentaorganosilicates **1**−**6**. These are best described as having polarized covalent bonds, which is in accord with the NMR spectroscopic large $J_{Si,C}$ coupling constants for **5** and **6**. The equatorial bonds have much stronger orbital interactions than the axial bonds, which are prone to heterolytic cleavage. The analyses show that the electron-withdrawing phenyl group stabilizes the axial bonds considerably. At the same time, the phenyl group is apico-indifferent due to a balance in repulsions between the phenyl π system and the silicate bonding orbitals. The bonding interaction increases with increasing number of phenyl substituents. However, even for triphenylsilicate **13** the axial Si−H bonds remain sensitive, as revealed in the reported X-ray structure, due to its close contact with the cation.[6a] Introduction of more phenyl groups is ineffective because of steric crowding between the axial phenyl groups and the *ortho*-hydrogen atoms of the equatorial phenyl groups. Therefore, silicates such as **2** are also of limited stability. The stability can be increased by reducing the size of the substituent and by enhancing its electron-withdrawing ability (and thus apicophilicity) as with trifluoromethyl groups in the reported silicate **4**.

A bidentate biaryl substituent provides electronic stabilization similar to that of two individual aryl groups. Thus, silicates such as **3** with a single ax,eq-biaryl moiety still have an axial group that is susceptible to dissociation, in line with experimental reports.[7a,b,d,9] A second biaryl group can be incorporated without causing congestion, as in **5** and **6**. Moreover, the conformer carrying one of the bidentates in a bisequatorial arrangement (**5A**) is disfavored by π repulsion and becomes the transition state for intramolecular ligand exchange. The methyl group of **5** is thus restricted to occupy an equatorial site, where it is much more strongly bound ($\Delta E_{int} = -111$; $\Delta E_{net} = 62$ kcal mol^{-1}) than in an axial position. This is consistent with the experimentally determined structures and pseudorotational barriers of the exceptionally stable, high-melting silicates **5** and **6**.[11b,30]

In conclusion, the presence of two sterically noninvasive bidentate biaryl moieties gives unique electronic stabilization to silicates that are conformationally restricted to prevent dissociation. Exploring this concept further may lead to novel highly stable pentaorganosilicates that may find applicability as weakly coordinating anions in ionic liquids and cationic catalyst systems.

Acknowledgment. This work has been supported by The Netherlands Organization for Scientific Research, Chemical Sciences (NWO-CW). We acknowledge the National Center for Computing Facilities (SARA) for computer time.

Supporting Information Available: Atomic coordinates and absolute energies of all calculated structures, details of π repulsion calculations, and complete ref 22. This material is available free of charge via the Internet at http://pubs.acs.org.

JA0645887

(29) The difference in slopes has a statistical rather than a physical meaning and is the result of two effects: (1) In the equatorially substituted silicates **8**-R, the Si−R bond is shorter than in the corresponding axially substituted **7**-R, and hence the electron-withdrawing effect of the substituent is more pronounced. As a consequence, ΔV_{elstat} covers a broader range for **8**-R, resulting in a steeper linear fit. (2) For **8**-R, the trend in the net bond strength ΔE_{net} of the axial Si−H bond is a combination of trends in ΔV_{elstat}, ΔE_{oi}, and the opposing ΔE_{Pauli}. All in all, ΔE_{net} covers a smaller range for **8**-R than for **7**-R, which further steepens the linear fit.

(30) Berry, R. S. *J. Chem. Phys.* **1960**, *32*, 933−938.
(31) Couzijn, E. P. A.; Ehlers, A. W.; Schakel, M.; Lammertsma, K., to be published.